SEE CORRECTION FOR THIS ARTICLE
PNAS RESEARCH ARTICLE | MICROBIOLOGY OPEN ACCESS

The surface interface and swimming motility influence surface-sensing responses in *Pseudomonas aeruginosa*

Xuhui Zheng[a], Emma J. Gomez-Rivas[a], Sabrina I. Lamont[b], Katayoun Daneshjoo[a], Angeli Shieh[a], Daniel J. Wozniak[b], and Matthew R. Parsek[a,1]

Edited by Thomas Silhavy, Princeton University, Princeton, NJ; received June 14, 2024; accepted August 1, 2024

Bacterial biofilms have been implicated in several chronic infections. After initial attachment, a critical first step in biofilm formation is a cell inducing a surface-sensing response. In the Gram-negative opportunistic pathogen *Pseudomonas aeruginosa*, two second messengers, cyclic diguanylate monophosphate (c-di-GMP) and cyclic adenosine monophosphate (cAMP), are produced by different surface-sensing mechanisms. However, given the disparate cellular behaviors regulated by these second messengers, how newly attached cells coordinate these pathways remains unclear. Some of the uncertainty relates to studies using different strains, experimental systems, and usually focusing on a single second messenger. In this study, we developed a tricolor reporter system to simultaneously gauge c-di-GMP and cAMP levels in single cells. Using PAO1, we show that c-di-GMP and cAMP are selectively activated in two commonly used experimental systems to study surface sensing. By further examining the conditions that differentiate a c-di-GMP or cAMP response, we demonstrate that an agarose–air interface activates cAMP signaling through type IV pili and the Pil-Chp system. However, a liquid–agarose interface favors the activation of c-di-GMP signaling. This response is dependent on flagellar motility and correlated with higher swimming speed. Collectively, this work indicates that c-di-GMP and cAMP signaling responses are dependent on the surface context.

surface sensing | c-di-GMP | cAMP | *Pseudomonas* | Biofilm

Significance

Surface sensing is a critical step for bacteria to establish colonization on various surfaces. This process elicits diverse responses, such as biofilm formation through c-di-GMP signaling, and pathogenicity and surface-associated twitching through cAMP signaling. These two distinct surface-sensing systems control divergent behaviors. At an air–surface interface, *Pseudomonas aeruginosa* employs the Pil-Chp system and type IV pili to sense the surface, leading to cAMP activation. Conversely, when an aqueous phase is present over the surface, the flagellar apparatus and c-di-GMP-mediated signaling is dominant. These findings emphasize the versatility of *P. aeruginosa* in responding to surfaces and suggest that *P. aeruginosa* tailors different surface behaviors to fit the environment.

Biofilms are cellular aggregates surrounded by an extracellular matrix that is composed of DNA, proteins, and exopolysaccharides (1, 2). The opportunistic pathogen *Pseudomonas aeruginosa* is a model species for studying biofilms in the laboratory and its ability to form biofilms has been associated with persistent infection (3). Biofilm formation begins with a free-swimming bacterium attaching to a surface. This signal is perceived by the bacterium in a process termed surface sensing (4, 5).

In *P. aeruginosa*, surface sensing can involve various signal transduction systems that respond to distinct types of surface-associated signals. These stimuli can elicit two major types of surface behaviors in attached bacteria, which are coordinated through the production of two intracellular signaling molecules, cyclic diguanylate monophosphate (c-di-GMP) and cyclic adenosine monophosphate (cAMP) (Fig. 1*A*). The production of c-di-GMP promotes the synthesis of biofilm matrix materials, leading to sessility, while cAMP favors virulence factor production and type IV pili (TFP)-mediated twitching motility, promoting surface exploration by the bacteria (6, 7). Not surprisingly, previous studies have demonstrated mutual antagonism between these two disparate signaling pathways (8, 9).

Activation of the c-di-GMP and cAMP surface-sensing signaling pathways is mediated by distinct mechanisms. A cAMP-inducing surface-sensing response involves the Pil-Chp chemosensory system and TFP. The interaction between TFP and the surface is perceived by the Pil-Chp system, perhaps through either the pili's adhesive tip protein, PilY1, and/or changes in inner membrane concentrations of the pilin subunit, PilA (10–14). Activation of the Pil-Chp system promotes cAMP production by stimulating activity of the major adenylate cyclase CyaB (15). In turn, cAMP stimulates the transcription of the Pil-Chp system, leading to twitching motility on the surface (7, 16).

Cell envelope stress is also generated through bacteria–surface interaction and can play a role in surface-sensing signal transduction (5, 17, 18). For example, surface contact can impact the integrity of periplasmic proteins, which activates the *P. aeruginosa* Wsp chemosensory system. This surface response leads to the activation of a diguanylate cyclase (DGC) WspR and subsequent c-di-GMP production (19). Notably, Wsp-mediated c-di-GMP production is activated heterogeneously within the attached cell population, suggesting that only a fraction of surface-associated cells commit to biofilm formation (20).

Finally, another surface-related signal involves flagellar interactions with a surface. The flagellar filament is an important surface attachment determinant, and bacteria encounter resistance to rotation and motion from their surrounding environment as

Author affiliations: [a]Department of Microbiology, University of Washington, Seattle, WA; and [b]Departments of Microbial Infection and Immunity, Microbiology, The Ohio State University, Columbus, OH

Author contributions: X.Z. and M.R.P. designed research; X.Z., E.J.G.-R., S.I.L., K.D., and A.S. performed research; X.Z. and M.R.P. contributed new reagents/analytic tools; X.Z., E.J.G.-R., and M.R.P. analyzed data; and X.Z., D.J.W., and M.R.P. wrote the paper.

The authors declare no competing interest.

This article is a PNAS Direct Submission.

[1]To whom correspondence may be addressed. Email: parsem@uw.edu.

This article contains supporting information online at https://www.pnas.org/lookup/suppl/doi:10.1073/pnas.2411981121/-/DCSupplemental.

Published September 16, 2024.

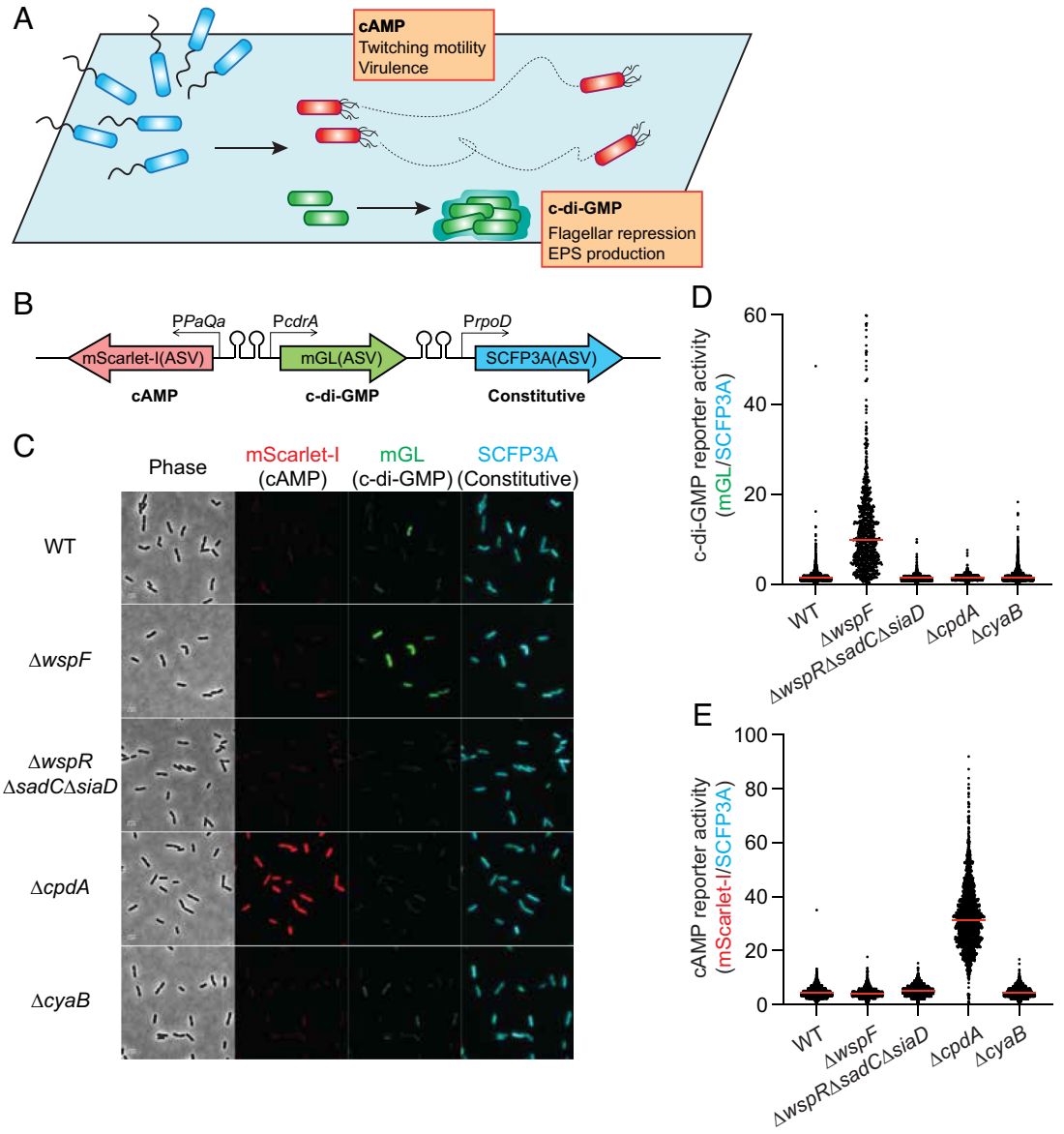

Fig. 1. A tricolor reporter system to measure c-di-GMP and cAMP. (*A*) *P. aeruginosa* may respond to a surface with activation of cAMP or c-di-GMP production. cAMP promotes type IV pili-mediated twitching motility and type III secretion system-mediated virulence. C-di-GMP promotes biofilm formation by repressing flagella and up-regulating the synthesis of biofilm matrix components. (*B*) Design of the tricolor reporter system. The promoter activity of the *PaQa* operon was used to represent cAMP levels, while the promoter activity of the *cdrA* gene reports c-di-GMP levels. The *rpoD* promoter activity represents a constitutive control. (*C*) Representative micrographs of reporter activity in the control strains during planktonic growth. (*D*-*E*) The c-di-GMP (*D*) or cAMP (*E*) reporter activity was calculated by normalizing the mean fluorescence intensity of the perspective channel to the constitutive channel in each bacterial cell. Each dot is a single cell. The horizontal red line represents the median reporter activity. The c-di-GMP or cAMP reporter activity in the subsequent figures was calculated in the same way, but only median reporter activity for each experiment was shown.

they swim via flagella (21–23). However, how flagellar-mediated surface sensing is transduced into an intracellular signal remains unclear, and different mechanisms have been proposed. When *P. aeruginosa* is tethered to the surface by the flagellum, increased flagellar load is suggested to induce cAMP production, which in turn alters flagellar function (24). Flagella–surface interactions are also implicated in c-di-GMP signaling. A flagellin mutant (Δ*fliC*) displays elevated levels of c-di-GMP when in contact with an agar surface. This phenotype could be reversed by the loss of MotAB stator, suggesting that both flagellin and MotAB are involved in the surface-regulated c-di-GMP signaling (25). In a separate study, MotAB, but not the flagellar filament, is crucial for the rapid c-di-GMP-responsive polar localization of FimW upon surface contact, suggesting that the flagellar motor-stator apparatus could act as a surface sensor (26).

To date, most studies have focused individually on the production of either c-di-GMP or cAMP surface-sensing systems. However, the different surface behaviors controlled by these signaling pathways elicit the question: How are these two signaling pathways coordinated in *P. aeruginosa*? Hypotheses have been put forth that c-di-GMP and cAMP are temporally activated (27). Additionally, the heterogeneity of c-di-GMP activation upon surface contact has raised the possibility that these two signaling pathways are selectively activated in different subpopulations of attached bacteria (20, 26, 28). It is also unclear how the nature of the surface impacts surface-sensing responses. Different experimental systems commonly utilized to study surface sensing, ranging from epithelial monolayers to bacteria tethered to beads by their flagella, may elicit a variety of cellular responses. To address the points listed above, we constructed and validated a tricolor

plasmid-based reporter system that monitors levels of c-di-GMP and cAMP simultaneously at a single-cell level. Using the *P. aeruginosa* strain PAO1, we found that two of the most widely used culturing systems to study surface sensing elicited starkly different signaling responses. An agarose pad favored a Pil-Chp-driven cAMP response, while attachment at a liquid–solid interface favored a c-di-GMP response. The c-di-GMP response required flagellar motility and implicated swimming speed as an important factor in surface sensing. Collectively, our data suggest that *P. aeruginosa* responds to different surface environments with distinct surface-sensing signaling pathways.

Results

Generation and Validation of a Tricolor Reporter System for Monitoring both c-di-GMP and cAMP Levels. To simultaneously assess the levels of c-di-GMP and cAMP in a single cell, we developed a reporter by integrating elements of the previously published c-di-GMP and cAMP transcriptional reporters, along with a constitutive promoter control (11, 29), leading to a tricolor plasmid-based system (Fig. 1*B* and *SI Appendix*, Fig. S1*A*). With this plasmid, the level of c-di-GMP is represented by the fluorescence intensity of a green fluorescent protein, mGreenLantern (mGL) (30), driven by the *cdrA* promoter. The level of cAMP is reflected by the fluorescence intensity of a red fluorescent protein, mScarlet-I (31), driven by the promoter of the *xphA-xqhA* operon *(PaQa)*. To normalize fluorescence intensity, we included SCFP3A, which is driven by the promoter of the *rpoD* housekeeping gene. To track the temporal dynamics of c-di-GMP and cAMP activity, all the fluorescent proteins were tagged with an AANDENYAASV short peptide (ASV-tag), which is a modified version of the *ssrA* tag, rendering fast turnover of these otherwise stable fluorescent proteins (stable for at least 960 min) (32) (*SI Appendix*, Fig. S1*B*). We have determined that the half-lives of these as ASV-tagged mGL, 89 ± 4 min; mScarlet-I, 149 ± 4 min; and SCFP3A, 45 ± 1 min (*SI Appendix*, Fig. S1*C*).

We first validated the sensitivity of our system by measuring reporter activity in bacterial strains with known phenotypic alterations in c-di-GMP/cAMP signaling. We assessed c-di-GMP reporter activity in a PAO1 Δ*wspF* mutant, which has a constitutively activated Wsp system and elevated cellular levels of c-di-GMP, as well as a Δ*wspR*Δ*sadC*Δ*siaD* triple mutant, which is deficient in c-di-GMP production due to loss of three active DGCs (33–36). To assess cAMP reporter activity, we used a PAO1 Δ*cpdA* mutant as a positive control, which is unable to degrade cellular cAMP through phosphodiesterase (PDE) activity (37). A PAO1 Δ*cyaB* mutant, lacking the major *P. aeruginosa* adenylate cyclase, served as a negative control (7). By microscopy, we observed comparable SCFP3A fluorescence across all planktonically grown strains. As expected, the Δ*wspF* mutant showed increased mGL fluorescence and the Δ*cpdA* mutant had increased mScarlet-I fluorescence (Fig. 1*C*). The reporter activity in wild-type (WT) was undifferentiable from the Δ*wspR*Δ*sadC*Δ*siaD* and Δ*cyaB* negative control strains, suggesting that the production of c-di-GMP and cAMP were low during planktonic growth (Fig. 1 *D* and *E*). As a control, we also constructed a promoterless control, which showed background fluorescence in each channel (*SI Appendix*, Fig. S2*A*).

We additionally compared reporter activity to cellular levels of c-di-GMP and cAMP quantitated by ELISA. Relative to WT, the PAO1 Δ*wspF* mutant displayed a 4.6-fold increase in c-di-GMP levels, corresponding to a 7.3-fold increased by the c-di-GMP reporter activity (*SI Appendix*, Fig. S2*B*). For cAMP, the 48.3-fold increase of cAMP in the Δ*cpdA* mutant strain correlated to a 7.4-fold increase in the cAMP reporter activity (*SI Appendix*, Fig. S2*C*).

Two Commonly used Model Systems Elicited Distinct and Specific Surface-Sensing Responses. To examine c-di-GMP and cAMP signaling in response to surfaces, we introduced PAO1 WT containing the tricolor reporter plasmid into two different surface-sensing model systems (Fig. 2*A*). These models have been previously used to study the mechanisms of surface-induced c-di-GMP and cAMP production (11, 20). In the first, planktonic bacteria were exposed to a glass coverslip in a flow cell for 10 min. We then monitored the activity of single cells by microscopy in the presence of flow. During the first 60 min following attachment, we observed a reduction in cell number, suggesting that many cells were only transiently associated with the coverslip surface (Fig. 2*B*). However, after 120 min, a subpopulation of cells exhibited an increased c-di-GMP reporter activity (Fig. 2*B* and Movie S1). After 4 h, the relative c-di-GMP reporter activity increased in the population, while the cAMP reporter activity remained relatively unchanged (Fig. 2*C*).

We also utilized an agarose pad model system of surface sensing. By contrast, this system elicited a steady increase of cAMP reporter activity (Fig. 2*D* and Movie S2). During the first 4 h of incubation on the agarose surface, c-di-GMP reporter activity dropped significantly (Fig. 2*E*). This is likely due to the dilution of fluorescence by cell division and degradation of the unstable fluorescent protein, although we can't rule out that there is a regulatory mechanism responsible for this decrease. Despite the dilution of fluorescence by cell division, the cAMP reporter activity in each cell increased over time (Fig. 2*E*). This agarose surface-induced cAMP response was dependent on the agarose concentration. At agarose concentrations that allow swimming motility (e.g., 0.3%), there was no increase in cAMP reporter activity. However, cAMP reporter activity was activated when the agarose concentration was >1% (*SI Appendix*, Fig. S3*A*). Collectively, these data suggest that the environmental context in which a surface is encountered determines the surface-sensing response.

The Agarose–Air Interface Favored cAMP Signaling and Type IV Pili Production. To identify environmental factors that might account for these different signaling outcomes, we tested the impact of experimental variables. This led us to identify that the key factor influencing the disparate activation of c-di-GMP and cAMP was the presence of a significant layer of liquid covering the surface. Thus, we established simplified model systems to make more direct comparisons (Fig. 3*A*). When planktonic bacteria were deposited directly on an agarose surface (agarose–air interface), surface-attached bacteria exhibited increased cAMP reporter activity and slightly lower c-di-GMP reporter activity (Fig. 3 *A* and *B*). In contrast, cells attached to the agarose–liquid interface had an increase in c-di-GMP reporter activity and unchanged cAMP reporter activity compared to the planktonic state (Fig. 3 *A* and *B*). Therefore, this simplified surface-sensing model recapitulated the phenotypes observed for the flow cell and agarose pad systems. cAMP signaling was induced when bacteria were isolated from the agarose–air interface but not the agarose–liquid interface (Fig. 3*C*). As expected, this response is dependent on CyaA and CyaB, two known adenylate cyclases responsible for synthesizing intracellular cAMP (Fig. 3*C*). To confirm these results, we replaced the *PaQa* promoter with *lacP1*, whose activity is also dependent on cAMP production (15). Like the *PaQa* promoter, the *lacP1* reporter also exhibited a significant CyaAB-dependent increase at the agarose–air interface (Fig. 3*D*). Unlike what has been

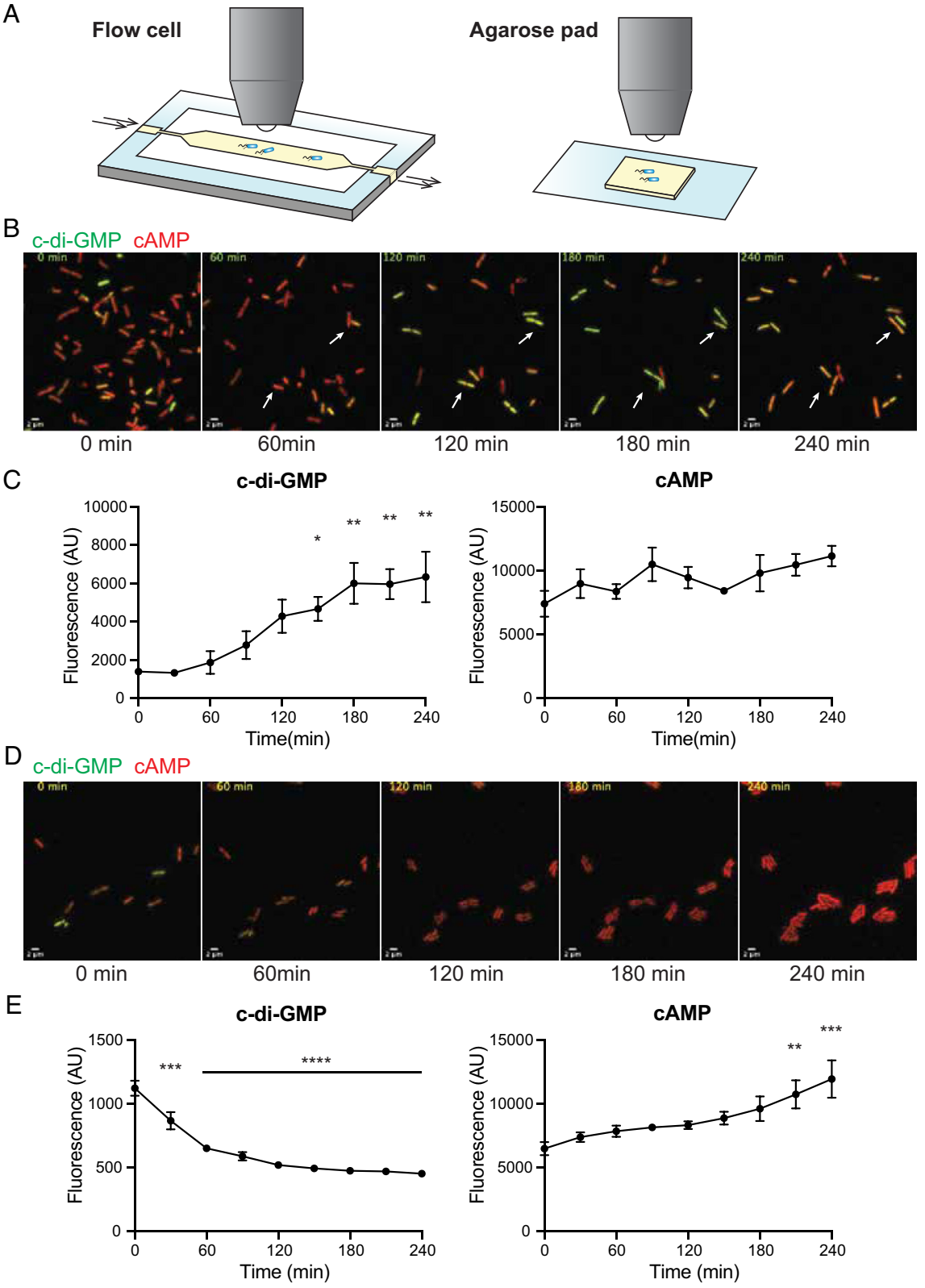

Fig. 2. Reporter activities in the flow cell and agarose pad models commonly used to study surface sensing. (*A*) Scheme of the experimental setups. In the flow cell model, bacteria were attached to a glass coverslip subjected to continuous liquid medium flow. In the agarose pad model, planktonic bacteria were deposited on the surface of a 1.5% agarose pad. (*B*) Time-lapse micrographs of bacteria taken at a single field of view at the glass surface of the flow cell, with 0 min representing initial attachment. White arrows indicate the cells showing a transition from low c-di-GMP reporter activity to high c-di-GMP reporter activity. (*C*) Quantification of the median single-cell fluorescence in the flow cell model. Data show mean ± SEM from three experiments. $*P < 0.05$, $**P < 0.01$ against 0 min by ordinary one-way ANOVA with Dunnett's multiple comparison test. (*D*) Time-lapse micrographs of bacteria on the surface of the agarose pad. Of note, the brightness and contrast in (*B*) and (*D*) were set differently to highlight the changes in each model system. (*E*) Quantification of the median single-cell fluorescence in the agarose pad model. Data show mean ± SEM from three experiments. $**P < 0.01$, $***P < 0.001$, $****P < 0.0001$ against 0 min by ordinary one-way ANOVA with Dunnett's multiple comparison test.

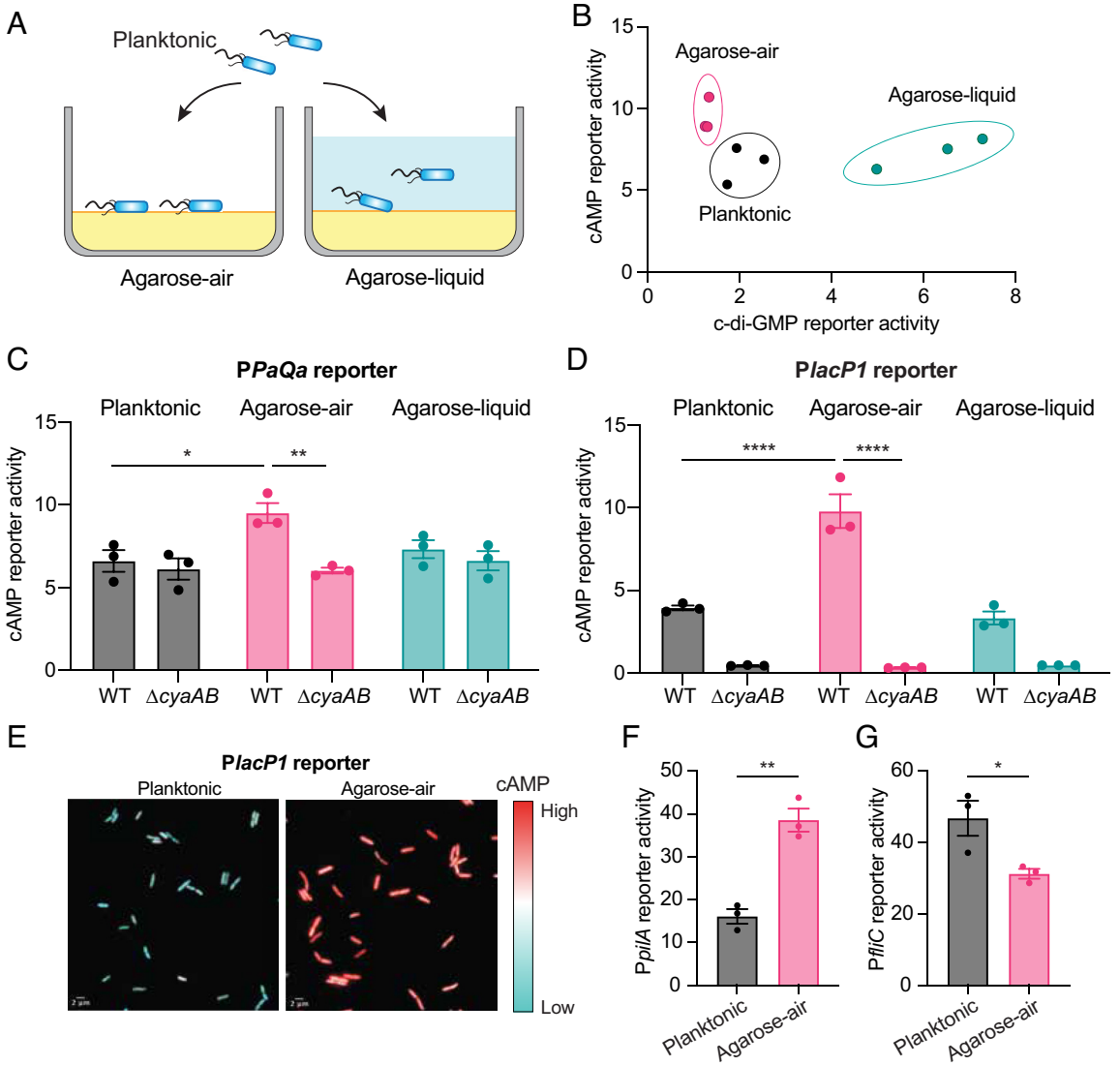

Fig. 3. The agarose–air interface activates cAMP signaling. (*A*) Depiction of the experimental system. Planktonic bacteria were added to the agarose surface directly (agarose-air) or as suspension in liquid (agarose–liquid). After 4 h of static incubation, surface-attached bacteria were collected and imaged for reporter activities. (*B*) Summary of the reporter activities after surface attachment of PAO1 WT. In the agarose–air condition, WT bacteria showed increased cAMP reporter activity, whereas in the agarose–liquid condition, WT bacteria exhibited increased c-di-GMP reporter activity. (*C*) Levels of cAMP measured by the promoter activity of the *PaQa* operon. Planktonic cells were imaged at mid-exponential growth. Agarose–air represents attached cells collected from the surface of the agarose–air system, and agarose–liquid represents attached cells taken from the agarose surface of that system. $*P < 0.05$, $**P < 0.01$ by ordinary one-way ANOVA with Tukey's multiple comparison test. (*D*) Levels of cAMP measured by the activity of the *lacP1* promoter. $****P < 0.0001$ by ordinary one-way ANOVA with Tukey's multiple comparison test. (*E*) Representative micrographs showing the relative cAMP reporter activity (red channel) and the constitutive promoter control (cyan channel) of WT during midexponential planktonic growth or agarose–air condition. (*F*) The expression of type IV pili in response to the agarose–air interface, measured by the promoter activity of the *pilA* gene. $**P < 0.01$ by a two-tailed *t* test. (*G*) The expression of flagella in response to the agarose–air interface, measured by the promoter activity of the *fliC* gene. $*P < 0.05$ by a two-tailed *t* test. (*B–D*, *F–G*) Each dot represents the median reporter activity across single cells in one experiment.

reported for surface-associated c-di-GMP signaling events (20), we observed a uniform response in cAMP reporter activity among individual cells with both the *lacP1* and *PaQa* reporter (Fig. 3*E* and *SI Appendix*, Fig. S3*B*). We also examined whether the surface response was reversible. To test this, we applied overlying liquid to bacteria initially inoculated to an air–agarose interface at different time points (*SI Appendix*, Fig. S4*A*). The total incubation time remained at 4 h. We found that if liquid medium was applied within the first hour, cells exhibited a c-di-GMP-dominated surface response (*SI Appendix*, Fig. S4*B*). Applying liquid at later time points favored a cAMP response (*SI Appendix*, Fig. S4*C*). This indicates that cells are not irreversibly committed to a cAMP response if the environmental conditions at the surface change.

Surface-induced cAMP production is dependent on TFP and the Pil-Chp chemosensory system (10, 11). Indeed, deletion of the gene encoding the major pilin subunit *pilA*, the extension ATPase *pilB*, the retraction ATPases *pilTU*, or the chemoreceptor of the Pil-Chp system *pilJ* each abolished surface-stimulated cAMP activation (*SI Appendix*, Fig. S3*C*). In accordance with previous studies, our data indicate that in the agarose–air interface, bacteria sense the surface via type IV pili and the Pil-Chp chemosensory system, thereby activating cAMP signaling.

To corroborate these findings, we used transcriptional reporters to monitor TFP and flagella gene expression. We observed increased *pilA* promoter activity and reduced *fliC* promoter activity in PAO1 WT cells attached to the agarose–air interface (Fig. 3 *F* and *G*). These results suggest that surface sensing at the agarose–air interface promoted type IV pili-mediated twitching motility while suppressing flagellar gene expression.

Surface Attachment Stimulates c-di-GMP Production at the Agarose–Liquid Interface. We next examined c-di-GMP signaling in surface-attached cells with the agarose–liquid system. The c-di-GMP reporter activity remained low in both planktonic culture and the interface of the agarose–air system. However, when bacteria were harvested from the surface of the agarose–liquid system, WT cells showed significantly increased c-di-GMP reporter activity (Fig. 4*A*). This increase in the cellular c-di-GMP level was also supported by ELISA to directly measure c-di-GMP in surface-attached cells (Fig. 4*B*). Similarly, we also examined whether the c-di-GMP surface response was reversible. To test this, we removed the overlying liquid at an agarose–liquid interface at different time points after inoculation to produce an agarose–air interface (*SI Appendix*, Fig. S5*A*). The total incubation time remained at 4 h. Similar to our data from the reverse experiment (*SI Appendix*, Fig. S4), we found that cells transitioned from a c-di-GMP to cAMP response when the surface environment changed (*SI Appendix*, Fig. S5 *B* and *C*).

Consistent with previous studies (20), the activation of c-di-GMP reporter activity was heterogeneous across single cells taken from the agarose–liquid interface (Fig. 4*C*). Based on the distribution of c-di-GMP reporter activity during planktonic culture, we arbitrarily set a threshold that considered 10% of planktonic WT cells as high c-di-GMP producers. Among the cells harvested from the agarose–liquid system, around 50% of WT cells showed c-di-GMP reporter activity above the threshold (Fig. 4*D*).

We also assessed TFP and flagellar gene expression in the cells associated with the agarose–liquid interface. While the *pilA* and *fliC* promoter activities were comparable to planktonic cells in the population (*SI Appendix*, Fig. S6 *A* and *B*), the high c-di-GMP subpopulation had lower *pilA* and *fliC* promoter activity compared to low c-di-GMP producers (*SI Appendix*, Fig. S6 *C* and *D*). These results suggest that c-di-GMP activation at the agarose–liquid interface led to an inhibition of both TFP and flagellum.

To further dissect the roles of different DGCs in surface-stimulated production of c-di-GMP, we examined the c-di-GMP reporter activity in individual PAO1 Δ*wspR,* Δ*sadC,* and Δ*siaD* mutant strains. Compared to WT, deletion of any individual DGC-encoding gene resulted in both a significant reduction in the percentage of cells with high c-di-GMP reporter activity and an overall reduction in the median c-di-GMP reporter activity across the total cell population (Fig. 4*D* and *SI Appendix*, Fig. S7). Among these mutants, the Δ*siaD* mutant exhibited the lowest percentage of cells with high c-di-GMP reporter activity (Fig. 4*D*). These data suggest that all three DGCs contribute to activation of c-di-GMP at the agarose–liquid interface.

Flagellar-Mediated Swimming Motility Is Critical for a c-di-GMP Surface-Sensing Response in the Agarose–Liquid System. We decided to further explore bacterial properties that influenced c-di-GMP signaling in the agarose–liquid system. We initially examined various mutant strains deficient in surface attachment. These include strains unable to make the biofilm matrix components such as polysaccharides Psl, Pel, alginate, type IV pili, and the matrix protein CdrA. None of these mutants significantly affected c-di-GMP reporter activity (*SI Appendix*, Fig. S8 *A* and *D*).

Due to the presence of a liquid layer, we hypothesized that swimming motility may influence signaling in the agarose–liquid system. In *P. aeruginosa*, the major flagellin subunit is encoded by *fliC*, and the rotation of the flagellar basal body is powered by two

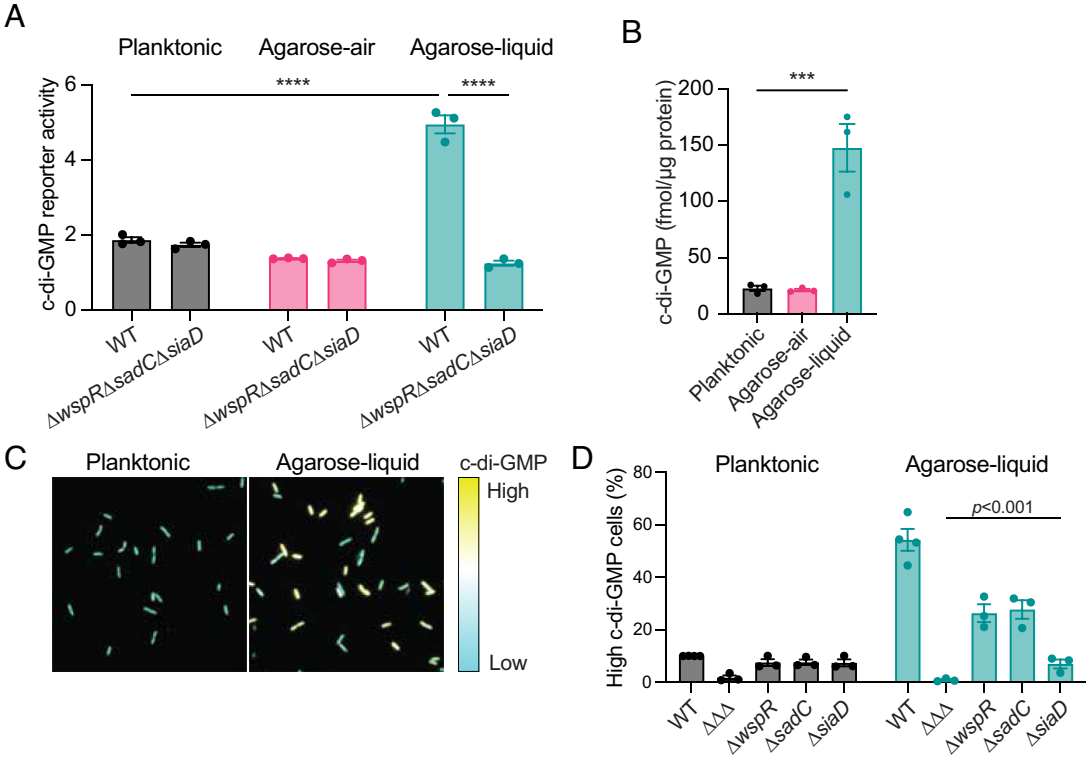

Fig. 4. Surface attachment of *P. aeruginosa* in the presence of liquid leads to c-di-GMP production. (*A*) The c-di-GMP reporter activity measured by the *cdrA* promoter activity. Each dot represents the median reporter activity across single cells in one experiment. ****$P < 0.0001$ by ordinary one-way ANOVA with Tukey's multiple comparison test. (*B*) Intracellular levels of c-di-GMP from different growth conditions indicated were measured by a c-di-GMP ELISA kit. Data show mean ± SEM from 3 experiments. ***$P < 0.0001$ by ordinary one-way ANOVA with Tukey's multiple comparison test. (*C*) Representative micrographs of WT cells taken from mid-exponential planktonic growth or attached cells from the agarose–liquid condition. The constitutive control is shown in the cyan channel and the c-di-GMP reporter activity is shown in the yellow channel. (*D*) Percentage of cells with high c-di-GMP reporter activity in planktonic or agarose–liquid growth conditions. Each dot represents the median reporter activity across single cells. Statistics comparing WT with individual mutants were performed using ordinary one-way ANOVA with Dunnett's multiple comparison test. ΔΔΔ, Δ*wspR*Δ*sadC*Δ*siaD*.

proton-coupled stators MotAB and MotCD (38, 39). These stators have been linked to surface sensing in *P. aeruginosa* (24–26). Additionally, the MotCD stator is needed to drive motility in viscous environments (39–41). We found that the Δ*fliC* and Δ*motAB* mutants lost the ability to activate c-di-GMP signaling in the agarose–liquid interface, while a Δ*motCD* mutant exhibited reduced signaling (Fig. 5*A* and *SI Appendix*, Fig. S9*A*). These phenotypes were complemented by reintroducing the gene(s) to the chromosome. These results suggest that flagellar-mediated swimming motility is critical for c-di-GMP production upon surface attachment.

To investigate the differential contribution of MotAB and MotCD to surface sensing, we first examined the roles of these stators in swimming motility under the conditions employed in the agarose–liquid system. In 0.3% agar swim plates, consistent with the phenotypes reported for *P. aeruginosa* strain PA14 and *Pseudomonas putida* (41, 42), MotCD was required for outward expansion from the inoculation point while MotAB was dispensable (*SI Appendix*, Fig. S9 *B* and *C*). However, the Δ*motAB* and Δ*motCD* mutant strains showed different swimming behavior in a liquid environment like that used in the agarose–liquid system (Movie S3–S5 and *SI Appendix*, Table S1). Most WT cells were observed to be motile (Movie S3). The Δ*motAB* mutant strain displayed a uniform reduction in swimming speed, with individual cells being able to swim and change directions (Movie S4). On the other hand, a subpopulation of Δ*motCD* cells failed to move during the period of measurement, while the cells that were moving swam as fast as WT (Movie 5). The impact of the *motAB* or *motCD* deletions was presented in a density plot showing the distribution of the swimming speed in any 0.1 s interval (Fig. 5*B*). Compared to WT, the Δ*motAB* mutant cells rarely exceeded speeds higher than about 30 μm/s (Fig. 5*B*). The Δ*motCD* mutant cells were able to swim fast as WT, but this occurred in a lower number of cells (Fig. 5*B* and *SI Appendix*, Fig. S9*D*, and Table S1).

Overall, we found that the MotAB stator was required for maximal swimming speeds (Fig. 5*C*). Since the Δ*motAB* mutant strain also had a more severe defect in c-di-GMP surface sensing than the Δ*motCD* mutant strain, we hypothesized that swimming speed might be an important parameter.

Environmental Conditions Influencing Swimming Speed Impacted c-di-GMP Surface-Sensing Signaling. One potential flagellar-dependent surface-sensing mechanism that could stimulate c-di-GMP is the stress/load placed on the flagellum due to surface contact. This mechanism is central to surface sensing in *Vibrio parahaemolyticus*, where the inability to spin the flagellum serves as an inducing signal for surface attachment (43). This work inspired us to investigate whether the addition of a viscosity agent could impede flagellar rotation and stimulate c-di-GMP signaling in *P. aeruginosa*. Ficoll is an inert and viscous reagent that has been used to arrest the swimming of bacteria (44, 45). At higher concentrations, the addition of Ficoll to planktonic cultures completely inhibited swimming (Fig. 5*D*, left Y axis, and Movie S6), presumably by impeding flagellar rotation. This impedance on swimming was homogenous across all cells, resulting in a decreased maximal speed as the concentration of Ficoll increased (*SI Appendix*, Fig. S10*A*). However, unlike *V. parahaemolyticus*, this increased load on the flagellum did not stimulate a surface-sensing response to produce more c-di-GMP (Fig. 5*D*, right Y-axis). These

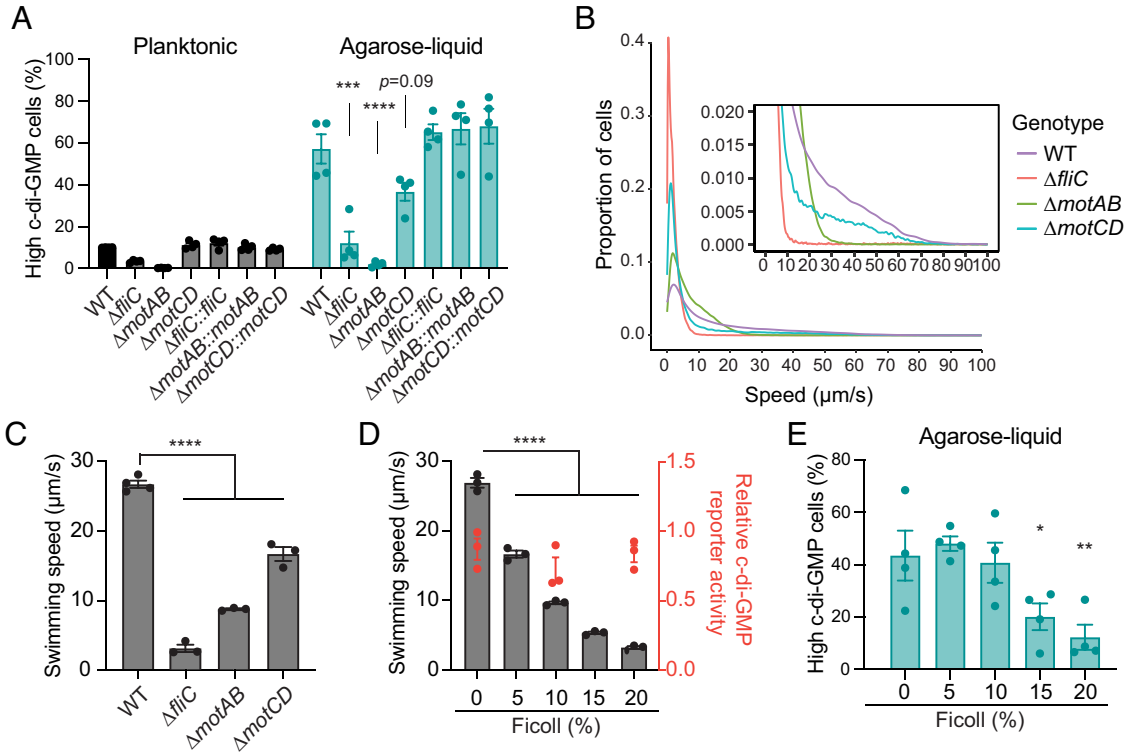

Fig. 5. Flagellar motility is critical for c-di-GMP signaling at the agarose–liquid interface. (*A*) The percentage of cells with high c-di-GMP reporter activity in indicated strains and conditions. The mutants were complemented by introducing the respective gene back to the native locus. ***$P < 0.001$, ****$P < 0.0001$ against WT by ordinary one-way ANOVA with Dunnett's multiple comparison test. (*B*) Density plot of the swimming speed in each 0.1 s interval of indicated strains. The inset shows the distribution of high swimming speed events. Data combined from 3 independent experiments. (*C*) The average swimming speed of indicated strains in the liquid medium. ****$P < 0.0001$ against WT by ordinary one-way ANOVA with Dunnett's multiple comparison test. (*D*) *Left* Y-axis: The average swimming speed of WT in the liquid medium containing different concentrations of Ficoll. ****$P < 0.0001$ against 0% Ficoll condition by ordinary one-way ANOVA with Dunnett's multiple comparison test. *Right* Y-axis: The median c-di-GMP reporter activity across single cells when mid-exponential PAO1 WT was exposed to different concentrations of Ficoll planktonically for 4 h. Data shown as relative c-di-GMP reporter activity normalized to the mid-exponential condition. (*E*) The percentage of cells with high c-di-GMP reporter activity when exposed to the agarose surface in the liquid medium containing different concentrations of Ficoll. *$P < 0.05$, **$P < 0.01$ against 0% Ficoll by ordinary one-way ANOVA with Dunnett's multiple comparison test.

data suggest that inhibition of flagellar rotation alone was insufficient to induce c-di-GMP signaling.

To examine whether swimming speeds influenced c-di-GMP activation, we modulated the swimming speed of WT by adding Ficoll to the liquid above the agarose surface in the agarose–liquid system. We found that the percentage of cells showing a c-di-GMP response significantly decreased in the presence of higher concentrations of Ficoll (Fig. 5*E* and *SI Appendix*, Fig. S10*B*). Since Ficoll also influences the density of the liquid environment, we examined the surface response in the presence of iodixanol, an agent that increases liquid density without having a pronounced effect on viscosity (46, 47). At concentrations of iodixanol that produce a similar density as Ficoll, there was a minimal effect on swim speeds (*SI Appendix*, Fig. S10*C*). We also did not observe a significant change of c-di-GMP reporter activity in the presence of iodixanol (*SI Appendix*, Fig. S10*D*).

Finally, we evaluated surface attachment of cells under these conditions. At the highest Ficoll concentration, there were a significant number of attached cells, even though c-di-GMP reporter activity was low (Fig. 5*E* and *SI Appendix*, Fig. S11). These data suggest that cells attaching to the surface is not sufficient to induce a c-di-GMP surface-sensing signaling response. However, we would like to note that bacteria still need to interact with the surface for a c-di-GMP response. In the case of the Δ*psl* mutant strain, it attached to a surface more poorly than WT (*SI Appendix*, Fig. S11). But it can still attach to a surface through other mechanisms, and those few cells that did attach produced a c-di-GMP response (*SI Appendix*, Fig. S8 *A* and *B*). Altogether, a c-di-GMP surface-sensing response requires both a surface and the ability of cells to swim or rotate their flagella at higher speeds toward or at the surface (Fig. 6).

Discussion

The second messengers c-di-GMP and cAMP are linked to surface sensing and control two distinct yet critical surface behaviors. In *P. aeruginosa*, both molecules are produced upon surface attachment, raising the question of how these two signaling pathways are coordinated to control surface behaviors. To directly address this question, we generated a tricolor reporter to simultaneously study c-di-GMP and cAMP surface signaling in individual cells. We initially tested our reporter in two *in vitro* surface-sensing models commonly used in the field. Our data indicate that production of either c-di-GMP or cAMP is influenced by the environment in which the surface is presented to cells. Specifically, an aqueous phase overlying the surface plays a crucial role in shaping surface-sensing responses (Fig. 6). We observed that cAMP signaling predominates at an air–solid interface. This surface-sensing response involves TFP and the Pil-Chp chemosensory system. By contrast, a c-di-GMP signaling response was observed on surfaces covered by an overlying liquid and this response requires flagellar motility. Collectively, our data suggest that surface sensing is environmentally contextual, potentially enabling bacteria to maximize fitness and surface colonization across diverse environments.

The agarose pad model system specifically promotes cAMP signaling, which is dependent on type IV pili and the Pil-Chp chemosensory system. This effect was influenced by the agarose concentration, with cAMP signaling diminished at lower concentrations (*SI Appendix*, Fig. S3*A*). This could be due to the influence of agar concentration on surface stiffness and/or pore size. By contrast, our agarose pad model system did not significantly induce c-di-GMP signaling. Laventie et al. suggest that when *P. aeruginosa* attaches to an agarose surface, there is a rapid, but brief increase of c-di-GMP within a few seconds before the increase of piliation (26). Using a transcriptional fusion, our reporter is probably not temporally sensitive enough to identify transient c-di-GMP or cAMP signaling events. However, our *pilA* reporter data indicate that the cells in this system are expressing type IV pili, a known downstream consequence of cAMP signaling (Fig. 3*G*). Furthermore, to address the strain specificity of surface sensing in *P. aeruginosa,* we also examined strain PA14 in our model systems. In PA14, the cAMP signaling was activated in the agarose–air interface similarly to PAO1, but to a lesser extent (*SI Appendix*, Fig. S12*A*). However, the c-di-GMP response was seen to be significantly delayed in the agarose–liquid system (*SI Appendix*, Fig. S12*B*). Another interesting aspect of cAMP signaling is that the response appears to be homogenous across the surface-associated population. This differs from c-di-GMP signaling, where the response is heterogeneous. The significance of this observation is unclear but may in part reflect the relative simplicity of the cAMP signaling network (i.e., involving only two cyclases and one PDE) as opposed to the c-di-GMP system with numerous DGCs and PDEs.

The presence of an aqueous phase overlying a surface promotes c-di-GMP signaling in PAO1. This is consistent with prior work from our group and others involving liquid–solid interfaces (20, 48, 49).

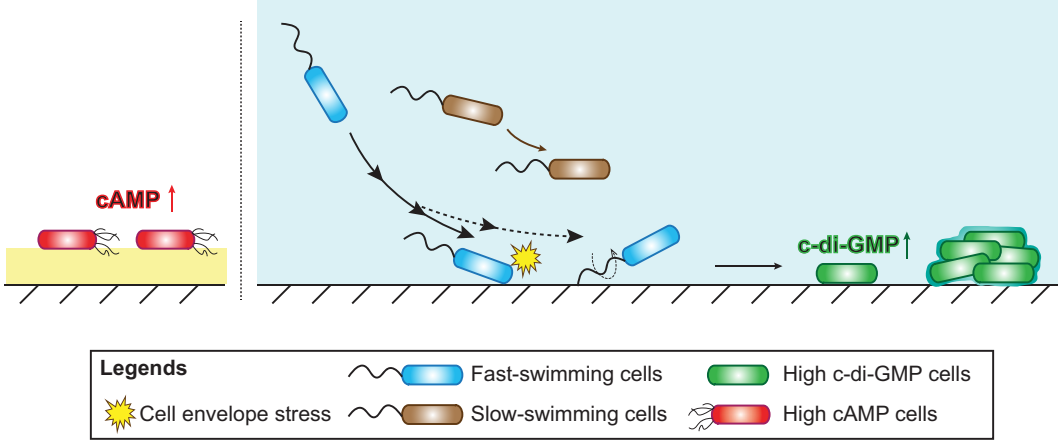

Fig. 6. Model of surface sensing in *P. aeruginosa*. When bacteria (red cells) attach to a porous surface that is directly exposed to air, bacteria sense the surface through type IV pili and thus activate cAMP signaling. When bacteria encounter a surface while in liquid, swimming motility is a critical factor to activate c-di-GMP signaling. We posit that the interaction between the fast swimmers (blue cells) with the surface may trigger cell envelope stress, leading to increased production of c-di-GMP (19). Alternatively, when bacteria are tethered with the surface through the flagellum, flagellar rotation may be a trigger for c-di-GMP production. Ultimately, activation of c-di-GMP signaling leads to aggregate formation. The slow-swimming cells (brown cells) cannot sense the surface to induce c-di-GMP synthesis.

A subset of surface-attached cells showed elevated c-di-GMP levels. As reported previously, this subpopulation is more likely to persist on the surface and become the founder cells of biofilm aggregates (20). Notably, while WspR, SadC, and SiaD are the primary DGCs contributing to the c-di-GMP pool, other DGCs thought to be involved in surface sensing, such as RoeA and GcbA, might be responsible for the small subset (<2%) of the population observed to have high c-di-GMP reporter activity in the *ΔwspRΔsadCΔsiaD* mutant (50, 51). One limitation of this system is that we do not know how long cells have been associated with the surface over the course of incubation. Cells that have adhered to the surface shortly before the 4 h point at which cells were harvested would not likely show a c-di-GMP response, resulting in an underestimation of c-di-GMP responses in individual cells.

Our data indicate that surface-stimulated c-di-GMP production requires bacteria to swim to the surface (Fig. 6). This is consistent with the models put forth by different groups suggesting the involvement of the flagellar apparatus in surface-sensing signal transduction (24, 26). Unlike *V. parahaemolyticus*, the surface-related signal transduced through the flagellum in *P. aeruginosa* does not simply involve an increased stress load placed on the motor-stator (Fig. 5*D*). Instead, we observed a clear correlation between swimming speed and surface-induced c-di-GMP production. The Δ*motAB* mutant was incapable of swimming at a faster speed or producing high levels of c-di-GMP, while the Δ*motCD* mutant reduced the occurrence of fast swimming events and produced less c-di-GMP. Likewise, the c-di-GMP signaling decreased when swimming speed was hindered by a liquid phase with increased viscosity (Fig. 5). This could be due to the need for swimming speed to either propel cells to where hydrodynamic interactions with the surface occur or maintain the appropriate angle of the cell approaching the surface (52, 53). The initial and transient interactions between a swimming bacterium and a surface likely produce cell envelope stress, which has been linked to the activity of WspR, SadC, and SiaD (19, 54–56). Another possibility is that in the case where there are initial attachment events involving flagellum–surface interactions, flagellar rotation at sufficient speeds produces the c-di-GMP response. Contribution of multiple DGCs to the c-di-GMP response suggests that cell envelope stress and flagellar/basal body signaling events may both be important. However, we should point out that in PAO1, attachment usually occurs along the body of the cell, with few cells remaining polarly attached via the flagellum, and those that do show reduced c-di-GMP signaling (20). While our simplified model was conducted under static conditions, studies have shown that flow can further increase c-di-GMP production, likely due to increased cell envelope stress derived from flow shear (49, 57). Furthermore, although surface sensing at the solid–liquid interface requires flagellar motility, a consequence of this signaling is for individual bacteria to stop moving and initiate biofilm formation (58).

Another interesting question raised by our results is whether the apparent lack of c-di-GMP signaling at an agarose–air interface means that c-di-GMP surface-sensing systems are not "sensing" the surface in this case. Our findings suggest that in the absence of swimming motility, c-di-GMP surface-sensing mechanisms are inactive at the agarose–air interface. Conversely, the lack of cAMP signaling seen at the agarose–liquid interface might suggest that this system is not actively perceiving the surface. This may be attributed to surface mechanics, as cAMP signaling is dependent on the agarose concentrations (*SI Appendix*, Fig. S3*A*) (12). In addition, published data suggest that these two signaling pathways can antagonize one another (8, 9). This makes sense in some regards. For example, biofilm matrix production induced by a c-di-GMP signaling surface-sensing response might hinder twitching motility induced by a cAMP surface-sensing response.

We also envision that, at an agarose–liquid interface, there is a greater fitness advantage to c-di-GMP signaling and the production of matrix components. This might help a subpopulation of cells adhere to the surface, preventing their removal from the surface by the hydrodynamic environment. On the surface without liquid such as the agarose–air interface described here, twitching motility provides a major fitness benefit by supporting surface exploration. When the % agarose is reduced to the point that flagellar-mediated motility can occur, the fitness benefit is lost. Production of matrix components via c-di-GMP signaling probably provides little benefit in an environment that favors twitching motility.

P. aeruginosa can colonize a variety of surfaces, from soil particles and water reservoirs in its natural habitat, to medical materials (catheters, implants, etc.) and host organs (59). The ability to differentiate between various surface environments and modulate surface-sensing signaling is a critical strategy for this bacterium to thrive in diverse environments. Our study highlights that the environmental context is a key determinant of the downstream signaling following surface sensing. While our model simply distinguishes the surface responses in the solid–air and solid–liquid interface in a rich medium, surface motility and biofilm structure in *P. aeruginosa* can be influenced by other environmental variables, such as nutritional conditions (60–64). Future studies will continue to address how *P. aeruginosa* surface sensing is regulated in complex environments. Understanding the mechanisms by which this motile-to-sessile phenotypic conversion occurs during initial stage of biofilm formation is vital to develop therapeutic strategies to eliminate or prevent the formation of bacterial biofilms, which continue to threaten the healthcare system.

Materials and Methods

Bacterial Strains and Growth Conditions. The strains and plasmids used in this study are listed in *SI Appendix*, Tables S2 and S3. *P. aeruginosa* strain PAO1 was used as the wild-type (WT) strain. *E. coli* and *P. aeruginosa* were routinely grown in LB (Lennox) broth at 37 °C with shaking at 225 rpm. *E. coli* strains were grown on LB (Lennox) agar, and *P. aeruginosa* were grown on LB (Lennox) agar or Pseudomonas isolation agar (PIA). When appropriate, 10 μg/ml gentamicin was supplemented for *E. coli* cultures, 30 or 100 μg/ml gentamicin was supplemented for *P. aeruginosa* cultures. Unless otherwise specified, *P. aeruginosa* were grown O/N at 37 °C before subculturing 1:100 (OD600 ~0.05) into fresh media. The subculture was collected after 3 h of growth (mid-exponential phase; OD600 ~0.5) as planktonic growth condition and used for further experiments.

Constructing Reporter Plasmids. The primers used in this study are listed in *SI Appendix*, Table S4. The mGreenLantern (mGL) protein (30) was codon-optimized for *P. aeruginosa* and synthesized with P*cdrA*-RBSII as a gBlock. The mScarlet-I and SCFP3A proteins were amplified from pEB2-mScarlet-I and pEB1-SCFP3A respectively (65). For all fluorescent proteins, the *ssrA* tag was added to the C terminus with two rounds of PCR: first, a peptide sequence of RPAANDENYA was added to the C terminus; second, the ASV peptide and overlap region with the vector was added to the C terminus. The promoter regions of *PaQa, rpoD, fliC,* and *pilA* were amplified from PAO1 genomic DNA. The *lacP1* promoter including the RNase III processing site was amplified from a previously reported cAMP reporter plasmid (15). PAO1 and PA14 share identical promoter sequences for *cdrA, PaQa,* and *rpoD* used in the reporter. The terminators T0 and T1 were amplified from pUC18Tmini-Tn7T-Gm, T2 from pEX18Gm, and Te from pUC18P-P*paqa*-YFP-P*rpoD*-mKate2 (11). The PCR fragments were assembled into the pBBR1MCS5 vector plasmid by HiFi Assembly. The sequences of the XZ198, XZ385, and XZ378 reporters can be found in Supplementary Text. The reporter plasmids were maintained in *E. coli* DH5a and electroporated into PAO1 WT and isogenic mutants for experiments.

Generating Mutant and Complement Strains. The PAO1 Δ*motAB,* Δ*motCD,* Δ*pilTU,* Δ*pilB,* and Δ*pilJ* mutants as well as the complementation of Δ*pilA,* Δ*fliC,* Δ*motAB,* and Δ*motCD* were generated using the allelic exchange system. For generating mutants, the flanking regions of the targeted genes were PCR amplified.

For complement strains, the flanking regions as well as the entire gene were PCR amplified. The amplicons were inserted into the pEX18Gm plasmid by HiFi Assembly. The plasmid was transformed into the *E. coli* S17.1 strain and subsequently into PAO1 via conjugation. The allelic exchange was performed as described previously (66). The targeted regions in the strains were confirmed by Sanger sequencing.

Time-Lapse Microscopy. The flow cell and agarose pad experiments were imaged with a Zeiss LSM 800 confocal laser scanning microscope to adapt to the setup of the flow cell system. For the flow cell experiment, the planktonic cells were diluted to OD600 ~0.1 with 1% LB and inoculated into a preassembled and sterilized flow cell. The bacteria were attached to the glass surface statically for 10 min before the flow of 1% LB was started. The flow rate was set to 5 rpm (~12 ml/h). For the agarose pad experiment, the planktonic cells were diluted to OD600 ~0.05 with FAB media (67). Of note, we have compared the agarose pad model made with LB and FAB media and observed cAMP-independent reporter activity in the LB medium; the c-di-GMP reporter activity remained the same in both media. A 2 μl drop was added to a pad made of 1.5% agarose in FAB + 30 mM glutamate and briefly air-dried. For both experiments, a z-stack of images were taken with a 100× objective every 5 min or 30 min as a 2 × 2 field (218.5 × 218.5 μm) for at least 4 h. The fluorescent channels of FITC (Ex 488 nm; Em 400 to 540 nm) and AF546 (Ex 561 nm; Em 576 to 700 nm) were used to image the mGL and mScarlet-I channels respectively. The brightfield was imaged through the ESID detector with a 640 nm laser.

Widefield Microscopy. The relative reporter activity was calculated from images taken with a Nikon Ti2 Eclipse inverted microscope. The collected cells were fixed with 2.5% paraformaldehyde (PFA) for 10 min at 37 °C. After washing away PFA, cells were stored in PBS and loaded onto a coverslip covered with a 1% agarose pad for imaging. The cells were imaged with a 100× objective using the phase contrast, and CFP, FITC, and TRITC filters (all with 10% laser power and 200 ms exposure time; CFP: Ex 438/24, Em 483/32; FITC: Ex 466/40, Em 525/50; TRITC: Ex 554/23, Em 609/54). At least 200 cells from two random fields were analyzed for each condition in an experiment.

Quantification of Fluorescence Intensity. The microscopy images were processed using the Fiji distribution of ImageJ and the plugin microbeJ (68, 69). For images taken with the widefield microscope, the phase contrast channel was used for identifying bacteria. The images were preprocessed to extract the local background and the Otsu method was used for thresholding. Bacteria were identified as rod-shaped particles with the same defined range of shape descriptors in all experiments. The background-extracted mean single-cell fluorescence intensity for all channels was exported and analyzed using R. The c-di-GMP or cAMP reporter activity was calculated as background-extracted mGL or mScarlet-I fluorescence divided by background-extracted SCFP3A fluorescence, respectively. For images taken with the confocal microscope, the images were z-projected to achieve the maximum fluorescence signal for the fluorescence channels. A single slice of the brightfield channel near the focal plane with dark bacteria and bright background was combined with the z-projected fluorescent channels and used for identifying single bacteria using microbeJ as described above. When reporting the relative reporter activity across the population, the median value of single cells was calculated for each channel. To calculate the percentage of cells with high c-di-GMP reporter activity, the planktonic WT population was arbitrarily determined to have 10% of high-c-di-GMP cells. This threshold was applied to all conditions in the same experiment.

Surface-Sensing Experiments in 24-Well Plates. Each well of the 24-well plate was filled with 1 ml of 1.5% agarose made in LB medium and the plate was air-dried for 1 h. The planktonic bacteria were pelleted and resuspended with 50% LB (LB diluted 1:1 with H_2O). For the agarose–air condition, 5 μl of bacteria was added to the agarose surface and air-dried for about 15 min. For the agarose–liquid condition, 1 ml of bacteria was added to the agarose surface. For the Ficoll and iodixanol experiments, bacteria were resuspended in media containing different concentrations of Ficoll 400 (Sigma-Aldrich) or iodixanol (Optiprep, Cosmo Bio). The volume of LB and H_2O was adjusted to ensure that LB was present in all conditions at 50%. The plate was incubated statically at 37 °C for 4 h. When the incubation is done, the liquid was removed from the agarose–liquid condition and the wells were rinsed gently with PBS twice. Surface-attached bacteria in both agarose–air and agarose–liquid conditions were fixed with 2.5% PFA at 37 °C for 10 min. The fixation was washed away, and the samples were stored in PBS at 4 °C until imaging.

Surface Attachment Measurement. To measure the percentage of surface-attached cells in the agarose–liquid condition, the 24-well plate was prepared and inoculated as described above. Two wells of the same strain were inoculated in each experiment. After 4 h of incubation, a well was washed as described above, and the surface-attached population was collected by rigorous resuspension in PBS. Another well was rigorously resuspended directly and collected as total cells. The number of cells in the surface-attached and total populations were enumerated by serial dilution and spot plating on a LB agar plate.

Swimming Assay on the Agar Plate. To evaluate the swimming motility in the agar plate, bacteria were inoculated into the center of 0.3% agar made in M9 medium (0.4% glucose) from a colony. The plates were incubated at 37 °C in a dampened environment to keep the agar concentration. The images were taken after 24 h of incubation using an Azure Imaging System with true color imaging and analyzed using Fiji. The swimming area was measured as a near-circle area in the middle of the plate that passed the brightness threshold.

Measuring Swimming Speed in Liquid Environment. To analyze the swimming motility in the liquid environment, we tracked the swimming trajectories under the microscope. The planktonic bacteria were normalized to OD600 ~0.1 with 50% LB to match the conditions in the surface-sensing experiments. If applicable, the 50% LB was supplemented with ficoll or iodixanol. Bacteria were added to a channel in μ-Slide VI 0.1 (Ibidi) and imaged with a Nikon Ti2 Eclipse microscope. The focal plane was chosen at the middle of the channel and phase contrast images were taken using a 40× objective every 0.1 s for 3 s. The images were analyzed with ImageJ plugin Trackmate (70). The swimming speed was calculated from all edges of bacterial movement in the 3 s timeframe.

Quantification of c-di-GMP and cAMP. The levels of c-di-GMP and cAMP were measured using c-di-GMP and cAMP ELISA kit (Cayman Chemical) following manufacture protocols. Bacteria were lysed with B-PER or 0.1 N HCl at room temperature for 10 min for c-di-GMP or cAMP quantification, respectively. The lysates were centrifuged to remove the cell debris at 14,000×g for 10 min at 4 °C. The supernatant was used for ELISAs or Qubit protein assays (ThermoFisher) to quantify protein concentrations.

Kinetics of Fluorescent Proteins. The parental untagged mGL, mScarlet-I, and SCFP3A and the *ssrA*-tag derivatives were cloned into the pJM220 plasmid (71) and electroporated into PAO1 WT. To measure the degradation of fluorescent proteins, bacteria were cultured O/N in FAB + 30 mM glutamate and subcultured at 1:25 dilution in FAB + 30 mM glutamate + 0.1% rhamnose until OD600 ~0.5. Bacteria were collected, washed twice with FAB, and resuspended in FAB without carbon source or rhamnose. The resuspension was added to a 96-well plate and the fluorescence intensity was measured every 10 min during 16 h incubation at 37 °C with shaking in a CLARIOstar Plus Plate reader (CFP: Ex 430/20, Em 480/20; mGL: Ex 490/10, Em 530/20; mScarlet-I: Ex 570/15, Em 613/20).

Statistical Analysis. All statistical analyses were performed in GraphPad Prism 9. Unless otherwise mentioned, each dot represents an independent experiment.

Data, Materials, and Software Availability. All study data are included in the article and/or Supporting Information.

ACKNOWLEDGMENTS. We thank the members of the Parsek laboratory for insightful discussions, and particularly Dr. Megan O'Malley for comments on this manuscript. We thank Dr. George O'Toole for comments on this manuscript, Dr. Alexandre Persat for the gift of pUC18P-P*paqa*-YFPP*rpoD*-mKate2 plasmid, Dr. Joe Harrison for the gift of plasmids for making some of the mutants, Dr. Georgia Squyres for the gift of rhamnose-inducible constructs and help for measuring the half-lives of fluorescent proteins, and Dr. Catherine Klancher for the gift of the P*lacP1* reporter plasmid. This study was supported by the National Institute of Health R01AI143916, R01AI077628, and R01AI134895 to D.J.W and M.R.P. This work was also supported in part by the Cure CF Columbus Translational Core (C3TC). C3TC is supported by the Division of Pediatric Pulmonary Medicine, the Biopathology Center Core, and the Data Collaboration Team at Nationwide Children's Hospital as part of the Research Development Program, Grant MCCOY19RO. X.Z. is a Cystic Fibrosis Foundation Awardee of the Life Sciences Research Foundation.

1. L. Hall-Stoodley, J. W. Costerton, P. Stoodley, Bacterial biofilms: from the natural environment to infectious diseases. *Nat. Rev. Microbiol.* **2**, 95–108 (2004).
2. R. M. Donlan, Biofilm formation: A clinically relevant microbiological process. *Clin. Infect. Dis.* **33**, 1387–1392 (2001).
3. M. F. Moradali, S. Ghods, B. H. A. Rehm, Pseudomonas aeruginosa lifestyle: A paradigm for adaptation, survival, and persistence. *Front Cell Infect. Microbiol.* **7**, 39 (2017).
4. B.-J. Laventie, U. Jenal, Surface sensing and adaptation in bacteria. *Annu. Rev. Microbiol.* **74**, 735–760 (2020).
5. T. E. P. Kimkes, M. Heinemann, How bacteria recognise and respond to surface contact. *FEMS Microbiol. Rev.* **44**, 106–122 (2020).
6. R. Simm, M. Morr, A. Kader, M. Nimtz, U. Römling, GGDEF and EAL domains inversely regulate cyclic di-GMP levels and transition from sessibility to motility. *Mol. Microbiol.* **53**, 1123–1134 (2004).
7. M. C. Wolfgang, V. T. Lee, M. E. Gilmore, S. Lory, Coordinate regulation of bacterial virulence genes by a novel adenylate cyclase-dependent signaling pathway. *Dev. Cell* **4**, 253–263 (2003).
8. H. Almblad *et al.*, High levels of cAMP inhibit Pseudomonas aeruginosa biofilm formation through reduction of the c-di-GMP content. *Microbiology (United Kingdom)* **165**, 324–333 (2019).
9. H. Almblad *et al.*, The cyclic AMP-Vfr signaling pathway in pseudomonas aeruginosa is inhibited by Cyclic Di-GMP. *J. Bacteriol.* **197**, 2190–2200 (2015).
10. Y. Luo *et al.*, A hierarchical cascade of second messengers regulates Pseudomonas aeruginosa Surface Behaviors. *mBio* **6**, e02456–14 (2015).
11. A. Persat, Y. F. Inclan, J. N. Engel, H. A. Stone, Z. Gitai, Type IV pili mechanochemically regulate virulence factors in Pseudomonas aeruginosa. *Proc. Natl. Acad. Sci. U.S.A.* **112**, 7563–7568 (2015).
12. M. D. Koch, M. E. Black, E. Han, J. W. Shaevitz, Z. Gitai, Pseudomonas aeruginosa distinguishes surfaces by stiffness using retraction of type IV pili. *Proc. Natl. Acad. Sci. U.S.A.* **119**, e2119434119 (2022).
13. S. L. Kuchma, G. A. O'Toole, Surface-induced cAMP signaling requires multiple features of the Pseudomonas aeruginosa Type IV Pili. *J. Bacteriol.* **204** (2022).
14. C. J. Geiger, G. A. O'Toole, Evidence for the type IV Pilus retraction motor PilT as a component of the surface sensing system in Pseudomonas aeruginosa. *J. Bacteriol.* **205**, e0017923 (2023).
15. N. B. Fulcher, P. M. Holliday, E. Klem, M. J. Cann, M. C. Wolfgang, The Pseudomonas aeruginosa Chp chemosensory system regulates intracellular cAMP levels by modulating adenylate cyclase activity. *Mol. Microbiol* **76**, 889–904 (2010).
16. J. J. Bertrand, J. T. West, J. N. Engel, Genetic analysis of the regulation of type IV pilus function by the Chp chemosensory system of Pseudomonas aeruginosa. *J. Bacteriol.* **192**, 994–1010 (2010).
17. K. Otto, T. J. Silhavy, Surface sensing and adhesion of Escherichia coli controlled by the Cpx-signaling pathway. *Proc. Natl. Acad. Sci. U.S.A.* **99**, 2287–2292 (2002).
18. R. M. Morgenstein, P. N. Rather, Role of the Umo proteins and the Rcs phosphorelay in the swarming motility of the wild type and an O-Antigen (waaL) Mutant of Proteus mirabilis. *J. Bacteriol.* **194**, 669–676 (2012).
19. L. O'Neal *et al.*, The Wsp system of Pseudomonas aeruginosa links surface sensing and cell envelope stress. *Proc. Natl. Acad. Sci. U.S.A.* **119**, e2117633119 (2022).
20. C. R. Armbruster *et al.*, Heterogeneity in surface sensing suggests a division of labor in Pseudomonas aeruginosa populations. *Elife* **8**, e45084 (2019).
21. G. A. O'Toole, R. Kolter, Flagellar and twitching motility are necessary for Pseudomonas aeruginosa biofilm development. *Mol. Microbiol.* **30**, 295–304 (1998).
22. J. C. Conrad *et al.*, Flagella and pili-mediated near-surface single-cell motility mechanisms in P. aeruginosa. *Biophys. J.* **100**, 1608–1616 (2011).
23. R. Chawla, R. Gupta, T. P. Lele, P. P. Lele, A skeptic's guide to bacterial mechanosensing. *J. Mol. Biol.* **432**, 523–533 (2020).
24. M. Schniederberend *et al.*, Modulation of flagellar rotation in surface-attached bacteria: A pathway for rapid surface-sensing after flagellar attachment. *PLoS Pathog.* **15**, e1008149 (2019).
25. J. J. Harrison *et al.*, Elevated exopolysaccharide levels in Pseudomonas aeruginosa flagellar mutants have implications for biofilm growth and chronic infections. *PLoS Genet.* **16**, e1008848 (2020).
26. B.-J. Laventie *et al.*, A surface-induced asymmetric program promotes tissue colonization by *Pseudomonas aeruginosa*. *Cell Host Microbe* **25**, 140–152.e6 (2019).
27. G. A. O'Toole, G. C. Wong, Sensational biofilms: Surface sensing in bacteria. *Curr. Opin. Microbiol.* **30**, 139–146 (2016).
28. C. K. Lee *et al.*, Multigenerational memory and adaptive adhesion in early bacterial biofilm communities. *Proc. Natl. Acad. Sci. U.S.A.* **115**, 4471–4476 (2018).
29. M. T. Rybtke *et al.*, Fluorescence-based reporter for gauging cyclic Di-GMP levels in Pseudomonas aeruginosa. *Appl. Environ. Microbiol.* **78**, 5060–5069 (2012).
30. B. C. Campbell *et al.*, mGreenLantern: A bright monomeric fluorescent protein with rapid expression and cell filling properties for neuronal imaging. *Proc. Natl. Acad. Sci. U.S.A.* **117**, 30710–30721 (2020).
31. D. S. Bindels *et al.*, MScarlet: A bright monomeric red fluorescent protein for cellular imaging. *Nat. Methods* **14**, 53–56 (2016).
32. J. B. Andersen *et al.*, New unstable variants of green fluorescent protein for studies of transient gene expression in bacteria. *Appl. Environ. Microbiol.* **64**, 2240–2246 (1998).
33. J. W. Hickman, D. F. Tifrea, C. S. Harwood, A chemosensory system that regulates biofilm formation through modulation of cyclic diguanylate levels. *Proc. Natl. Acad. Sci. U.S.A.* **102**, 14422–14427 (2005).
34. M. Valentini, A. Filloux, Biofilms and Cyclic di-GMP (c-di-GMP) Signaling: Lessons from Pseudomonas aeruginosa and Other Bacteria. *J. Biol. Chem.* **291**, 12547–12555 (2016).
35. J. H. Merritt, K. M. Brothers, S. L. Kuchma, G. A. O'Toole, SadC reciprocally influences biofilm formation and swarming motility via modulation of exopolysaccharide production and flagellar function. *J. Bacteriol.* **189**, 8154–8164 (2007).
36. G. Chen *et al.*, The SiaA/B/C/D signaling network regulates biofilm formation in Pseudomonas aeruginosa. *EMBO J.* **39**, e103412 (2020).
37. E. L. Fuchs *et al.*, In vitro and in vivo characterization of the Pseudomonas aeruginosa Cyclic AMP (cAMP) phosphodiesterase CpdA, required for cAMP homeostasis and virulence factor regulation. *J. Bacteriol.* **192**, 2779–2790 (2010).
38. T. B. Doyle, A. C. Hawkins, L. L. McCarter, The complex flagellar torque generator of Pseudomonas aeruginosa. *J. Bacteriol.* **186**, 6341–6350 (2004).
39. C. M. Toutain, M. E. Zegans, G. A. O'Toole, Evidence for two flagellar stators and their role in the motility of Pseudomonas aeruginosa. *J. Bacteriol.* **187**, 771–777 (2005).
40. A. E. Baker *et al.*, Flagellar stators stimulate c-di-GMP production by Pseudomonas aeruginosa. *J. Bacteriol.* **201**, e00741–18 (2019).
41. S. L. Kuchma *et al.*, Cyclic di-GMP-mediated repression of swarming motility by Pseudomonas aeruginosa PA14 Requires the MotAB stator. *J. Bacteriol.* **197**, 420–430 (2015).
42. V. Pfeifer, S. Beier, Z. Alirezaeizanjani, C. Beta, Role of the two flagellar stators in swimming motility of Pseudomonas putida. *mBio* **13**, e0218222 (2022).
43. L. McCarter, M. Hilmen, M. Silverman, Flagellar dynamometer controls swarmer cell differentiation of V. parahaemolyticus. *Cell* **54**, 345–351 (1988).
44. V. A. Martinez *et al.*, Flagellated bacterial motility in polymer solutions. *Proc. Natl. Acad. Sci. U.S.A.* **111**, 17771–17776 (2014).
45. S. Kamdar *et al.*, The colloidal nature of complex fluids enhances bacterial motility. *Nature* **603**, 819–823 (2022).
46. E. Martínez-Salas, J. A. Martín, M. Vicente, Relationship of Escherichia coli density to growth rate and cell age. *J. Bacteriol.* **147**, 97–100 (1981).
47. N. Bellotto *et al.*, Dependence of diffusion in Escherichia coli cytoplasm on protein size, environmental conditions, and cell growth. *Elife* **11**, e82654 (2022).
48. C. K. Lee *et al.*, Broadcasting of amplitude- and frequency-modulated c-di-GMP signals facilitates cooperative surface commitment in bacterial lineages. *Proc. Natl. Acad. Sci. U.S.A.* **119**, e2112226119 (2022).
49. C. A. Rodesney *et al.*, Mechanosensing of shear by Pseudomonas aeruginosa leads to increased levels of the cyclic-di-GMP signal initiating biofilm development. *Proc. Natl. Acad. Sci. U.S.A.* **114**, 5906–5911 (2017).
50. J. H. Merritt *et al.*, Specific control of Pseudomonas aeruginosa surfaceassociated behaviors by two c-di-GMP diguanylate cyclases. *mBio* **1**, e00183-10 (2010).
51. O. E. Petrova, K. E. Cherny, K. Sauer, The Pseudomonas aeruginosa diguanylate cyclase GcbA, a homolog of P. Fluorescens GcbA, promotes initial attachment to surfaces, but not biofilm formation, via regulation of motility. *J. Bacteriol.* **196**, 2827–2841 (2014).
52. A. P. Berke, L. Turner, H. C. Berg, E. Lauga, Hydrodynamic attraction of swimming microorganisms by surfaces. *Phys. Rev. Lett.* **101**, 038102 (2008).
53. G. Li, J. X. Tang, Accumulation of microswimmers near a surface mediated by collision and rotational Brownian motion. *Phys. Rev. Lett.* **103**, 078101 (2009).
54. K. A. Lewis *et al.*, "Ethanol decreases pseudomonas aeruginosa flagellar motility through the regulation of flagellar stators in J" in *Bacteriol* (American Society for Microbiology, 2019).
55. J. Klebensberger, A. Birkenmaier, R. Geffers, S. Kjelleberg, B. Philipp, SiaA and SiaD are essential for inducing autoaggregation as a specific response to detergent stress in Pseudomonas aeruginosa. *Environ. Microbiol.* **11**, 3073–3086 (2009).
56. A. I. Chen *et al.*, Candida albicans ethanol stimulates Pseudomonas aeruginosa WspR-controlled biofilm formation as part of a cyclic relationship involving phenazines. *PLoS Pathog.* **10**, e1004480 (2014).
57. S. Lecuyer *et al.*, Shear stress increases the residence time of adhesion of Pseudomonas aeruginosa. *Biophys. J.* **100**, 341–350 (2011).
58. U. Jenal, A. Reinders, C. Lori, Cyclic di-GMP: Second messenger extraordinaire. *Nat. Rev. Microbiol.* **15**, 271–284 (2017).
59. M. R. Parsek, P. K. Singh, Bacterial biofilms: An emerging link to disease pathogenesis. *Annu. Rev. Microbiol.* **57**, 677–701 (2003).
60. J. D. Shrout *et al.*, The impact of quorum sensing and swarming motility on Pseudomonas aeruginosa biofilm formation is nutritionally conditional. *Mol. Microbiol.* **62**, 1264–1277 (2006).
61. S. Sauvage *et al.*, Impact of carbon source supplementations on Pseudomonas aeruginosa physiology. *J. Proteome Res.* **21**, 1392–1407 (2022).
62. D. D. Sriramulu, H. Lünsdorf, J. S. Lam, U. Römling, Microcolony formation: A novel biofilm model of Pseudomonas aeruginosa for the cystic fibrosis lung. *J. Med. Microbiol.* **54**, 667–676 (2005).
63. M. Klausen *et al.*, Biofilm formation by Pseudomonas aeruginosa wild type, flagella and type IV pili mutants. *Mol. Microbiol.* **48**, 1511–1524 (2003).
64. T. Köhler, L. K. Curty, F. Barja, C. van Delden, J.-C. Pechère, Swarming of Pseudomonas aeruginosa is dependent on cell-to-cell signaling and requires flagella and pili. *J. Bacteriol.* **182**, 5990–5996 (2000).
65. E. Balleza, J. M. Kim, P. Cluzel, Systematic characterization of maturation time of fluorescent proteins in living cells. *Nat. Methods* **15**, 47–51 (2018).
66. L. R. Hmelo *et al.*, Precision-engineering the Pseudomonas aeruginosa genome with two-step allelic exchange. *Nat. Protoc.* **10**, 1820–1841 (2015).
67. A. Heydorn *et al.*, Quantification of biofilm structures by the novel computer program comstat. *Microbiology (NY)* **146**, 2395–2407 (2000).
68. J. Schindelin *et al.*, Fiji: An open-source platform for biological-image analysis. *Nat. Methods* **9**, 676–682 (2012).
69. A. Ducret, E. M. Quardokus, Y. V. Brun, MicrobeJ, a tool for high throughput bacterial cell detection and quantitative analysis. *Nat. Microbiol.* **1**, 16077 (2016).
70. J. Y. Tinevez *et al.*, TrackMate: An open and extensible platform for single-particle tracking. *Methods* **115**, 80–90 (2017).
71. J. Meisner, J. B. Goldberg, The Escherichia coli rhaSR-PrhaBAD inducible promoter system allows tightly controlled gene expression over a wide range in Pseudomonas aeruginosa. *Appl. Environ. Microbiol.* **82**, 6715–6727 (2016).